

# Paramagnetic relaxivity of delocalized long-lived states of protons in chains of CH<sub>2</sub> groups

Aiky Razanahoera, Anna Sonnefeld, Geoffrey Bodenhausen, Kirill Sheberstov

Department of chemistry, École Normale Supérieure, PSL University, 75005 Paris, France

5 *Correspondence to:* Kirill Sheberstov, kirill.sheberstov@ens.psl.eu

**Abstract.** Long-lived states (LLS) have lifetimes  $T_{LLS}$  that can be much longer than longitudinal relaxation times  $T_1$ . In molecules containing several geminal pairs of protons in neighbouring CH<sub>2</sub> groups, it has been shown that *delocalized* LLS can be excited by converting magnetization into imbalances between the populations of singlet and triplet states of each pair. Since the empirical yield of the conversion and reconversion of observable magnetization into LLS and back is on the order of 10% if one uses spin-locked induced crossing (SLIC), it would be desirable to boost the sensitivity by dissolution dynamic nuclear polarization (d-DNP). To enhance the magnetization of nuclear spins by d-DNP, the analytes must be mixed with radicals such as 4-hydroxy-2,2,6,6-tetramethylpiperidin-1-oxyl (TEMPO). After dissolution, these radicals lead to an undesirable paramagnetic relaxation enhancement (PRE) which shortens not only the longitudinal relaxation times  $T_1$  but also the lifetimes  $T_{LLS}$  of LLS. It is shown in this work that PRE by TEMPO is less deleterious for LLS than for longitudinal magnetization, for four different molecules: 2,2-dimethyl-2-silapentane-5-sulfonate (DSS), homotaurine, taurine, and acetylcholine. The relaxivities  $r_{LLS}$  (i.e., the slopes of the relaxation rate constants  $R_{LLS}$  as a function of the radical concentration) are 3 to 5 times smaller than the relaxivities  $r_1$  of longitudinal magnetization. Partial delocalization of the LLS across neighbouring CH<sub>2</sub> groups may decrease this advantage, but in practice, this effect was observed to be small, for example when comparing taurine containing two CH<sub>2</sub> groups and homotaurine with three CH<sub>2</sub> groups. Regardless of whether the LLS are delocalized or not, it is shown that PRE should not be a major problem for experiments combining d-DNP and LLS, provided the concentration of paramagnetic species after dissolution does not exceed 1 mM, a condition that is readily fulfilled in typical d-DNP experiments. In bullet d-DNP experiments however, it may be necessary to decrease the concentration of TEMPO or to add ascorbate for chemical reduction.

## Introduction

25 The lifetime of spin state populations in nuclear magnetic resonance (NMR) is normally limited by longitudinal relaxation. In certain cases, it is possible to access spin states that have extended lifetimes. In coupled pairs of spins with  $I = \frac{1}{2}$ , such long-lived states (LLS) correspond to population imbalances between singlet and triplet states (Carravetta and Levitt, 2004; Carravetta et al., 2004) that are immune to intra-pair dipole-dipole interactions, which for pairs of protons are normally the dominant cause of longitudinal relaxation. In larger systems, LLS may involve four, six or more spins, all these states are

30 weakly affected by dipolar relaxation (Hogben et al., 2011). The relaxation time constants  $T_{LLS}$  can be much longer than typical longitudinal relaxation time constants  $T_1$ . This feature is particularly useful for protein-ligand studies (Salvi et al., 2012; Buratto et al., 2014b, 2016). Applications of LLS can be combined with different hyperpolarization methods, such as parahydrogen-based methods (Franzoni et al., 2012) or dissolution dynamic nuclear polarization (d-DNP) (Bornet et al., 2014; Kiryutin et al., 2019). D-DNP is the most universal method to achieve high spin polarization, and has found applications in drug screening  
35 (Lee et al., 2012; Buratto et al., 2014a; Kim et al., 2016), and in studies of metabolism by *in-vivo* magnetic resonance imaging (MRI) (Nelson et al., 2013). Before dissolution, the saturation of the electron spin transitions by micro-wave irradiation of a solid sample near 1 K leads to an enhancement of the nuclear spin polarization by up to 4 orders of magnitude, compared to the thermal polarization at room temperature in the same magnetic field. The sample is then quickly dissolved and transferred to a solution-state NMR spectrometer, where the high-resolution spectrum is observed (Ardenkjær-Larsen et al., 2003). In an  
40 alternative approach known as “bullet DNP”, the cold solid sample is ejected from the polarizer and rapidly transferred to the NMR spectrometer where it is dissolved (Kouřil et al., 2019). After dissolution, the unpaired electrons of the dilute paramagnetic agent give rise to undesirable paramagnetic relaxation enhancement (PRE). For most molecules of interest, such as metabolites or potential drugs, proton relaxation is fast so that the level of hyperpolarization suffers during dissolution and transfer, which is one of the reasons why d-DNP is more often used for  $^{13}\text{C}$  or  $^{15}\text{N}$  rather than for protons. Although molecules  
45 that are in enriched  $^{13}\text{C}$  and  $^{15}\text{N}$  offer many possibilities for the excitation of LLS (Feng et al., 2013; Elliott et al., 2019; Sheberstov et al., 2019), there are several drawbacks of using heteronuclei. Labelled compounds are expensive and  $^{13}\text{C}$  or  $^{15}\text{N}$  observation is much less sensitive compared to  $^1\text{H}$ . After converting proton LLS back into proton magnetization, only proton signals of interest are observed, while the background is suppressed. LLS involving pairs of protons often provide good contrast because protons are often directly exposed to the drug/target interface. On the other hand, the relaxation rate constants of LLS  
50 can be enhanced by mechanisms such as dipolar couplings to solvent nuclei, even with low gyromagnetic ratios, and to paramagnetic species (Kharkov et al., 2022).

Recently it was discovered that LLS involving geminal pairs of protons can be readily excited in many molecules containing at least two neighboring  $\text{CH}_2$  groups (Sonnefeld et al., 2022a, b). Aliphatic chains, which are the focus of this study, are commonly found in potential drugs, so that LLS of  $\text{CH}_2$  groups could provide a new tool for drug screening using NMR.  
55 Hyphenation of LLS methodology with d-DNP offers promising perspectives, since at very low spin temperatures on the order of 10 mK that are routinely achieved in d-DNP, singlet-triplet imbalances can result from a violation of the high-temperature approximation, so that LLS can be excited without any radio-frequency (RF) irradiation (Tayler et al., 2012; Bornet et al., 2014; Kress et al., 2019). LLS that involve chemically equivalent proton pairs in  $\text{CH}_2$  groups need not be sustained by RF fields or protected by shuttling to low fields. Therefore, one can transfer samples with hyperpolarized LLS to an NMR  
60 spectrometer for detection without significant losses of polarization. For small molecules, the ratios  $T_{LLS}/T_1$  range typically from 2 to 6 for LLS in  $\text{CH}_2$  groups in non-degassed samples (Sonnefeld et al., 2022a) although in some degassed samples containing isolated pairs of protons (Sarkar et al., 2007) or carbon-13 nuclei (Pileio et al., 2012; Stevanato et al., 2015) it is possible to achieve ratios  $T_{LLS}/T_1 > 30$ . In this work, we carried out a systematic analysis of relaxivities, i.e., of the dependence

of the relaxation rate constants of LLS and longitudinal magnetization on the concentration of the paramagnetic species 4-hydroxy-2,2,6,6-tetramethylpiperidin-1-oxyl (TEMPO).

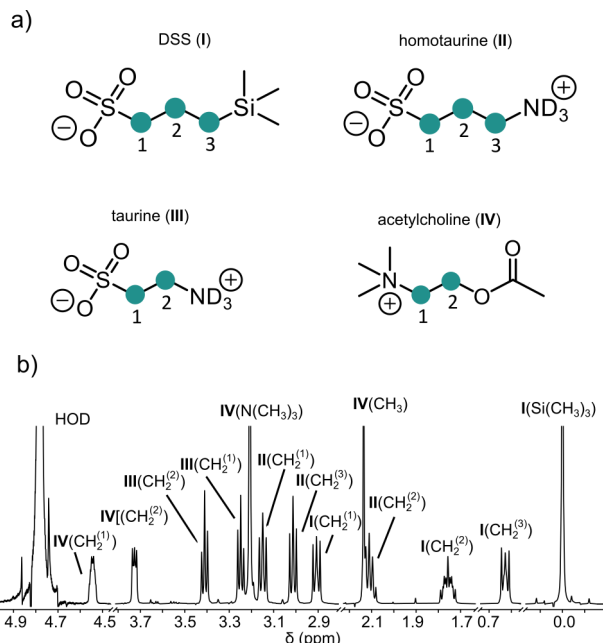


**Figure 1. (a) Chemical structures of four molecules supporting LLS of CH<sub>2</sub> groups studied in this work: 2,2-Dimethyl-2-silapentane-5-sulfonate sodium salt (DSS, I), homotaurine (II), taurine (III), acetylcholine (IV). CH<sub>2</sub> groups supporting LLS are numbered in each structure and highlighted by green circles. (b) Assignment of the <sup>1</sup>H NMR spectrum of a mixture containing all four compounds.**

Paramagnetic transition metal ions (Cu<sup>2+</sup>, Mn<sup>2+</sup>), lanthanides (Gd<sup>3+</sup>) and triplet oxygen (O<sub>2</sub>) have been shown to induce PRE of LLS, although PRE is not very efficient because the fluctuating external fields at the sites of two closely-spaced protons attached to the same carbon atom are strongly correlated (Tayler and Levitt, 2011). The effects of triplet oxygen on LLS have been investigated in detail (Erriah and Elliott, 2019). The question arises if fluctuating external fields due to the bulky TEMPO radical are more strongly correlated than for paramagnetic ions or oxygen, in particular when they act on delocalized LLS involving several neighbouring CH<sub>2</sub> groups in the molecules shown in Figure 1. In DSS (I) and homotaurine (II), the LLS can be delocalized over all six protons of the three CH<sub>2</sub> groups, whereas in taurine (III) and acetylcholine (IV) the LLS always involves all four protons of both CH<sub>2</sub> groups. Titration experiments with TEMPO allowed us to determine to what extent the radical affects the LLS lifetimes and to determine whether it is necessary to quench the radicals after dissolution (Miéville et al., 2010). In low fields, in particular after dissolution during the transfer between the polarizer and the NMR magnet, PRE may be exacerbated by translational diffusion (Borah and Bryant, 1981) of the paramagnetic molecules relative to the analytes (Miéville et al., 2011).

## Experimental methods

The delocalised LLS were excited by using spin-lock induced crossing (SLIC) (DeVience et al., 2013) and its  
 85 polychromatic extension (Sonnefeld et al., 2022b). A generic SLIC pulse sequence is illustrated in Figure 2a. After a non-  
 selective  $90^\circ$  pulse that rotates the magnetization into the transverse plane, one, two or three continuous SLIC pulses with a  
 common duration  $\tau_{SLIC}$  are applied to the nuclei of interest, with a common RF amplitude (nutating frequency)  $\nu_1$  that matches  
 a multiple of the geminal intra-pair  $J$ -coupling, i.e.,  $\nu_1 = n J^{intra}_{HH}$  with  $n = 1$  for double- and  $n = 2$  for single-quantum SLIC.  
 Level anti-crossings (LACs) lead to a transfer of magnetization into LLS, i.e., into a population imbalance between states with  
 90 different permutation symmetry. Since pairs of protons in  $CH_2$  groups are chemically equivalent in achiral molecules (i.e., have  
 the same chemical shifts), and, in the absence of couplings to heteronuclei, are often nearly magnetically equivalent, there is  
 no need to suppress singlet-to-triplet leakage by transporting the sample into a region of low magnetic field, or by applying an  
 RF field to sustain the imbalance. After allowing the LLS to relax during a delay  $\tau_{rel}$ , a  $T_{00}$  filter removes shorted-lived terms  
 (Tayler and Levitt, 2013; Tayler, 2020), and a second SLIC pulse reconverts the remaining LLS back into observable  
 95 magnetization for detection. In this work, SLIC experiments with single, double, and triple irradiation (henceforth called  
 “single, double, and triple SLIC experiments” for simplicity) were carried out to determine  $T_{LLS}$ , as shown by wavy arrows in  
 Figure 2b and c.

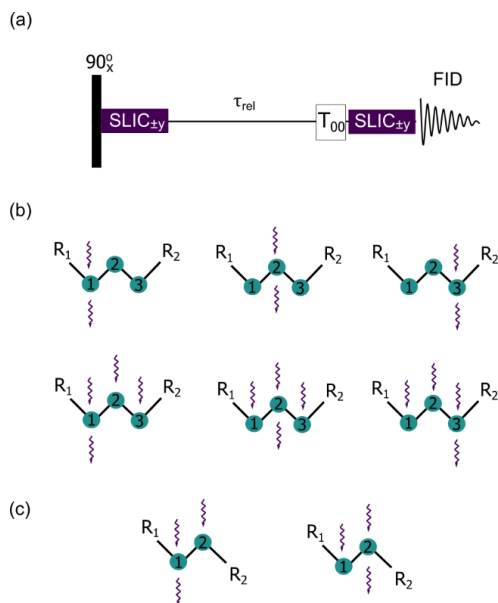
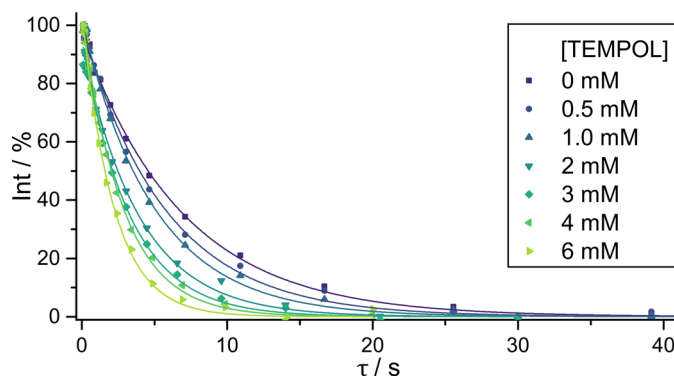


**Figure 2. (a) Generic pulse sequence for single- and poly- spin-lock induced crossing (SLIC) where selective RF fields can be applied simultaneously to two or more  $CH_2$  groups. (b) Six possible poly-SLIC experiments applied to molecules containing three  $CH_2$  groups such as I and II of Fig. 1a. The upper row shows three experiments with irradiation at a single frequency for the creation of LLS and a single readout pulse applied to the offset of the first, second or third  $CH_2$  group; the lower row shows three experiments using triple irradiation of all three  $CH_2$  groups for LLS excitation, combined with a single readout SLIC applied to only one of the three  $CH_2$  groups. (c) Two schemes with double SLIC excitation and single SLIC readout for compounds containing only two  $CH_2$  groups such as III and IV of Fig. 1a.**

100 Titrations were performed by preparing a set of samples where all compounds except TEMPOL had fixed concentrations. The volume of each sample was 600  $\mu$ L. A stock solution with 40 mM of each compound was diluted by a factor 4 to obtain a final concentration of 10 mM for each compound in  $D_2O$  at pH 7.0 without removing paramagnetic oxygen by degassing. A stock solution of phosphate buffer (70 mM  $KH_2PO_4$  and 130 mM  $K_2HPO_4$ ) was prepared in  $D_2O$  and diluted by factor 4. A 20 mM TEMPOL stock solution was diluted in steps and added to yield final concentrations of 0.5, 1.0, 2.0, 3.0, 4.0, and 6.0 mM. The  $^1H$  NMR spectra were obtained by adding 16 signals (for experiments with single SLIC irradiation) or

8 signals (for experiments with multiple SLIC irradiation) using a 500 MHz AVANCE Neo Bruker spectrometer with a 5mm  
 105 iProbe at 298 K. Each sample contained a mixture of all four molecules, thus ensuring accurate comparisons of relaxation rate  
 constants of different molecules. The  $^1\text{H}$  NMR spectrum of the mixture with its assignments is presented in Figure 1b. Typical  
 signal decays due to LLS relaxation as a function of the TEMPOL concentration are shown in Figure 3. The intensities of the  
 LLS-derived signals are typically about 5 % for single SLIC experiments and up to 10 % for poly-SLIC experiments. The  
 theoretical maximum efficiency of LLS excitation and reconversion in a four-spin  $-\text{CH}_2-\text{CH}_2-$  moiety was calculated to be  
 110 14% for single SLIC and 28% for double SLIC experiments (Sonnefeld et al., 2022a). Simulations of the contributions of  
 different LLS terms to the observed signals were performed using SpinDynamica (Bengs and Levitt, 2018).



115 **Figure 3.** Decays of LLS-derived signals of DSS (compound I) for different TEMPOL concentrations. The LLS were excited and  
 reconverted by irradiation with single SLIC pulses applied to  $\text{CH}_2^{(1)}$  with an RF amplitude of 27 Hz to match the condition for single-  
 quantum level anti-crossing (SQ LAC). The solid lines correspond to mono-exponential fits, scaled to begin at 100%.

## Results and discussion

### 1.1 Comparison of relaxivities of long-lived states and of longitudinal magnetization: partly correlated random fields

As apparent in Figure 4, both the longitudinal relaxation rate constant  $R_1 = 1/T_1$  and the long-lived relaxation rate  
 constant  $R_{LLS} = 1/T_{LLS}$  depend linearly on the concentration of TEMPOL (in units of M or mol/L):

$$\begin{aligned} R_1 &= R_1^{(0)} + r_1 [\text{TEMPOL}], \\ R_{LLS} &= R_{LLS}^{(0)} + r_{LLS} [\text{TEMPOL}]. \end{aligned} \quad (1)$$

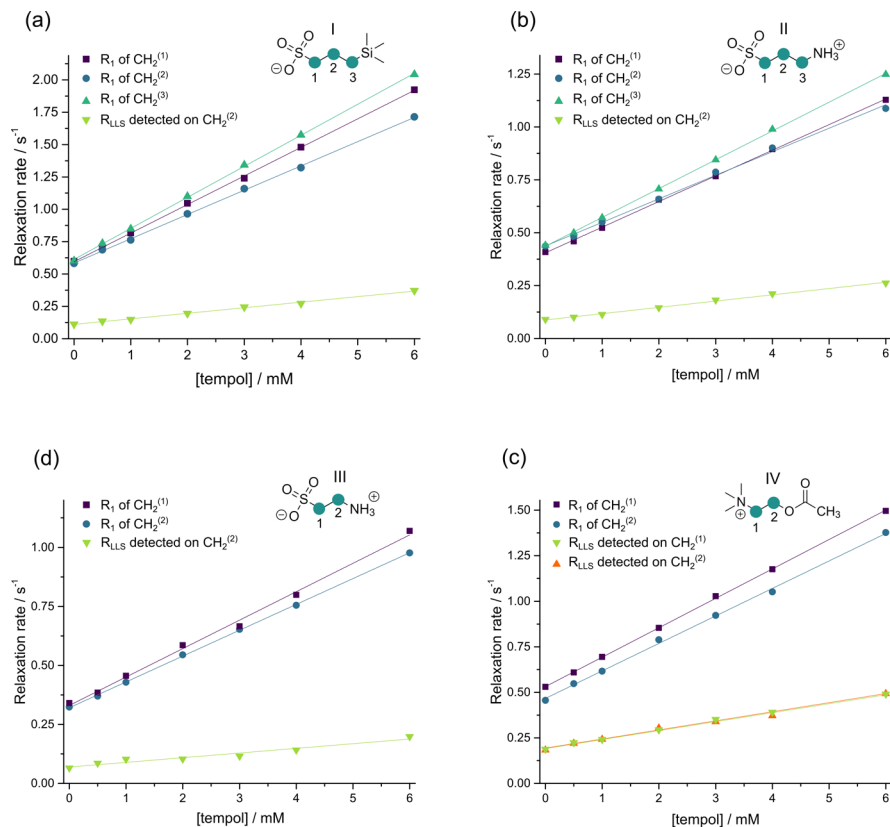
120 The slopes  $r_{LLS}$  and  $r_1$  are known as *relaxivities* (in units of  $\text{M}^{-1}\text{s}^{-1}$ ); the intercepts  $R_1^{(0)}$  and  $R_{LLS}^{(0)}$  are the rate constants determined  
 in the absence of TEMPOL. Figure 4 shows that variations of  $R_1$  between neighboring  $\text{CH}_2$  groups within each molecule are  
 much smaller than variations from one molecule to another. Whereas the  $T_1$  values of small molecules correlate with the  
 molecular mass – the larger molecule, the shorter  $T_1$  – this is not true for  $T_{LLS}$ . In the absence of TEMPOL, the longest  $T_{LLS}$  of  
 ca. 15 s was observed for compound III, whereas the shortest  $T_{LLS}$  of ca. 5 s was found for compound IV, although their  $T_1$

125 relaxation times and molecular masses are roughly the same, so that their correlation times should be similar. The difference of  $T_{LLS}$  may be explained by the presence of 12 methyl protons in compound IV, which cause faster relaxation of LLS.

Wokaun and Ernst famously demonstrated that PRE is less efficient for relaxation of zero-quantum coherences than for single- and double-quantum coherences (Wokaun and Ernst, 1978). Tayler and Levitt demonstrated that a similar logic also applies to LLS: whereas longitudinal relaxation is enhanced by fluctuations of external local fields induced by unpaired  
130 electrons of radicals, an LLS involving two spins  $\vec{I}_1$  and  $\vec{I}_2$  is only relaxed by fluctuating external fields if these are *not* correlated. In general, the extent of correlation of the two fluctuating fields at the locations of the two spins  $\vec{I}_1$  and  $\vec{I}_2$  can be characterized by the correlation coefficient  $C = \langle \vec{B}_1 \cdot \vec{B}_2 \rangle / (B_1 B_2)$ , where  $B_i = \sqrt{\langle \vec{B}_i \cdot \vec{B}_i \rangle}$  is the mean (time-averaged) amplitude. Only the *uncorrelated* part of the two fluctuating fields given by  $\langle \vec{B}_1 - \vec{B}_2 \rangle^2 = (B_1^2 + B_2^2 - 2\langle \vec{B}_1 \cdot \vec{B}_2 \rangle)$  contributes effectively to LLS relaxation (Tayler and Levitt, 2011). The smaller the radical, the closer it can approach one of the two  
135 geminal protons, hence the smaller the correlation coefficient  $C$ . It has been shown (Tayler and Levitt, 2011) that the ratio of relaxivities:

$$\kappa = r_{LLS}/r_1, \tag{2}$$

is a characteristic measure of the correlation coefficient  $C$ ; the smaller  $\kappa$ , the larger  $C$ . The experimental ratios  $\kappa$  for the (chemically inequivalent) protons of the  $\text{CH}_2$  group in the (chiral) dipeptide alanine-glycine varied in the range  $0.5 < \kappa < 0.3$  depending on the size of the paramagnetic agent (Tayler and Levitt, 2011). A similar ratio  $\kappa = 0.36$  was observed for the  $\text{CH}_2$   
140 group in the terminal glycine residue of the tripeptide Ala-Gly-Gly for PRE caused by triplet oxygen (Erriah and Elliott, 2019).



145 **Figure 4. Relaxation rate constants  $R_1 = 1/T_1$  and  $R_{LLS} = 1/T_{LLS}$  in  $\text{CH}_2$  groups of the four molecules I-IV as a function of the TEMPOL concentration. In (a) and (b), the LLS were excited by triple SLIC, in (c) and (d) by double SLIC, both with an RF amplitude of 13.5 Hz to match the condition for double-quantum level anti-crossing (DQ LAC.) In all cases, the LLS were reconverted into magnetization by single SLIC applied to the  $\text{CH}_2^{(2)}$  group, except for compound IV, where two sets of experiments were performed with reversion into magnetization of either  $\text{CH}_2^{(1)}$  or  $\text{CH}_2^{(2)}$  groups. The relaxivities  $r_1$  and  $r_{LLS}$  correspond to the slopes of the linear regressions.**

150 In  $\text{CH}_2$  chains with chemically equivalent pairs of protons in achiral molecules excited by exploiting magnetic inequivalence, the LLS can be delocalized over several  $\text{CH}_2$  groups. Relaxation of an LLS localized within an individual  $\text{CH}_2$  group will contribute to the decay of a delocalized LLS, so that one may expect the relaxivity of delocalized LLS to be more strongly affected by PRE than the relaxivity of a (hypothetical) localized LLS. We must however remain cautious, all the more since the longitudinal magnetizations of individual  $\text{CH}_2$  groups may have a different relaxivities  $r_1$ . As we shall discuss below,

155 the variations in the observed relaxivities  $r_{LLS}$  are not very large for different combinations of excitation and reconversion methods, and intramolecular variations are much smaller than differences between distinct compounds, so that one can estimate an average ratio of relaxivities  $\langle \kappa \rangle = \langle r_1 \rangle / \langle r_{LLS} \rangle$  for all  $\text{CH}_2$  groups in a given molecule. Compounds I-IV feature average ratios  $\langle \kappa_I \rangle \approx 0.22$ ,  $\langle \kappa_{II} \rangle \approx 0.23$ ,  $\langle \kappa_{III} \rangle \approx 0.18$ , and  $\langle \kappa_{IV} \rangle \approx 0.32$  (see Table 1). Note the similarity of the ratios  $\langle \kappa_{II} \rangle$  and  $\langle \kappa_{III} \rangle$

obtained for compounds that differ by only one CH<sub>2</sub> group. The LLS can be delocalized to a variable extent between all three  
 160 CH<sub>2</sub> groups in I and II, but are always equally distributed between the two CH<sub>2</sub> groups in compounds III and IV.

**Table 1. Experimentally determined relaxation rate constants (s<sup>-1</sup>) and relaxivities (M<sup>-1</sup>s<sup>-1</sup>). Standard errors determined from linear  
 regressions are shown in parentheses. For double SLIC, the RF amplitude was chosen to match the condition for double-quantum  
 level anti-crossing (LAC), leading to different imbalances characterized by different rate constants  $R_{LLS}^{(0)}(SQ)$  with single SLIC  
 165 excitation and single SLIC reconversion, and to rate constants  $R_{LLS}^{(0)}(DQ)$  with triple SLIC excitation and single SLIC reconversion.**

Compound	$R_1^{(0)}$	$R_{LLS}^{(0)}(SQ)$	$R_{LLS}^{(0)}(DQ)$	$r_1$	$r_{LLS}(SQ)$	$r_{LLS}(DQ)$
<b>I, CH<sub>2</sub><sup>(1)</sup></b>	0.596(6)	0.144(2)	0.111(4)	0.221(2)	0.051(1)	0.043(1)
<b>I, CH<sub>2</sub><sup>(2)</sup></b>	0.585(6)	0.116(2)	0.106(3)	0.188(2)	0.046(1)	0.045(1)
<b>I, CH<sub>2</sub><sup>(3)</sup></b>	0.613(5)	0.125(3)	0.113(2)	0.240(2)	0.054(1)	0.048(1)
<b>II, CH<sub>2</sub><sup>(1)</sup></b>	0.405(4)	0.120(2)	0.093(3)	0.121(1)	0.029(1)	0.022(1)
<b>II, CH<sub>2</sub><sup>(2)</sup></b>	0.438(9)	0.102(3)	0.088(3)	0.111(3)	0.032(1)	0.030(1)
<b>II, CH<sub>2</sub><sup>(3)</sup></b>	0.437(3)	0.114(7)	0.089(3)	0.136(1)	0.032(2)	0.022(1)
<b>III, CH<sub>2</sub><sup>(1)</sup></b>	0.33(1)	-	-	0.120(3)	-	-
<b>III, CH<sub>2</sub><sup>(2)</sup></b>	0.321(3)	-	0.069(7)	0.109(1)	-	0.020(2)
<b>IV, CH<sub>2</sub><sup>(1)</sup></b>	0.532(4)	-	0.194(3)	0.162(1)	-	0.050(1)
<b>IV, CH<sub>2</sub><sup>(2)</sup></b>	0.467(8)	-	0.191(6)	0.151(3)	-	0.049(2)

## 1.2 Implications for dissolution DNP

Even though delocalized LLS are less affected by TEMPOL than longitudinal magnetization, the observed decrease in  $T_{LLS}$  is  
 undesirable in the context of d-DNP. Since the use of TEMPOL or other polarizing agents is mandatory for d-DNP  
 170 experiments, the question arises if it is worth scavenging TEMPOL after dissolution by addition of a reducing agent such as  
 sodium ascorbate (vitamin C) to extend  $T_{LLS}$  after dissolution (Miéville et al., 2010, 2011). Note that the preparation of samples  
 comprising two types of beads is rather cumbersome, in particular for bullet DNP. According to Miéville et al., the rate of the  
 reduction of TEMPOL by sodium ascorbate may be slow on the time-scale of the transfer of the dissolved sample from the  
 polarizer to the NMR magnet. Hence the reaction may not be entirely completed by the time the sample arrives in the  
 175 spectrometer. Scavenging by sodium ascorbate may be accelerated ca. 100 times if one uses Frémy's salt instead of TEMPOL  
 (Negroni et al., 2022). Several alternative approaches have been developed to remove radicals once DNP has been achieved.  
 One approach is to use radicals obtained by UV irradiation of frozen pyruvic acid. These radicals are quenched as soon as the  
 temperature increases (Eichhorn et al., 2013). One may also use radicals grafted onto mesostructured silica materials (Gajan  
 et al., 2014) or microporous polymers (Ji et al., 2017; El Daraï et al., 2021). However, the small relaxivities presented in Table  
 180 1 suggest that scavenging may not be necessary when using LLS to preserve the hyperpolarization.



### 1.3 Experiments and simulations for molecules with three CH<sub>2</sub> groups

It was shown (Sonnefeld et al., 2022b) that for the excitation of LLS in systems with  $n = 3$  neighboring CH<sub>2</sub> groups, i.e., with  $2n = 6$  spins, there are 7 orthogonal LLS product operators that can be created, with 7 coefficients  $\lambda_i$  that depend on the excitation scheme:

$$\begin{aligned} \hat{\sigma}_{LLS} = & (-\lambda_{AA'} \hat{\mathbf{I}}^A \cdot \hat{\mathbf{I}}^{A'} - \lambda_{MM'} \hat{\mathbf{I}}^M \cdot \hat{\mathbf{I}}^{M'} - \lambda_{XX'} \hat{\mathbf{I}}^X \cdot \hat{\mathbf{I}}^{X'}) \\ & [-\lambda_{AA'MM'} (\hat{\mathbf{I}}^A \cdot \hat{\mathbf{I}}^{A'}) (\hat{\mathbf{I}}^M \cdot \hat{\mathbf{I}}^{M'}) - \lambda_{AA'XX'} (\hat{\mathbf{I}}^A \cdot \hat{\mathbf{I}}^{A'}) (\hat{\mathbf{I}}^X \cdot \hat{\mathbf{I}}^{X'}) - \lambda_{MM'XX'} (\hat{\mathbf{I}}^M \cdot \hat{\mathbf{I}}^{M'}) (\hat{\mathbf{I}}^X \cdot \hat{\mathbf{I}}^{X'})] \\ & - \lambda_{AA'MM'XX'} (\hat{\mathbf{I}}^A \cdot \hat{\mathbf{I}}^{A'}) (\hat{\mathbf{I}}^M \cdot \hat{\mathbf{I}}^{M'}) (\hat{\mathbf{I}}^X \cdot \hat{\mathbf{I}}^{X'}), \end{aligned} \quad (3)$$

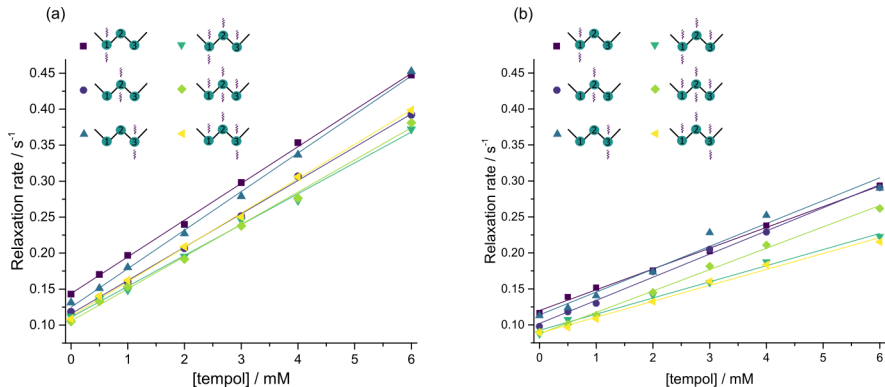
185 Here A and A' denote the two protons of the CH<sub>2</sub><sup>(1)</sup> group, M and M' those of the middle CH<sub>2</sub><sup>(2)</sup> group, while X and X' correspond to the terminal CH<sub>2</sub><sup>(3)</sup> group. This equation gives a general form of the density operator obtained after poly-SLIC, containing all long-lived terms found by numerical solution of the Liouville-von-Neumann equation. In addition to three bilinear terms, one encounters four higher terms that contain products of 4 and 6 spin operators. In principle, each term in Eq. (3) can decay with a different rate constant, so that one could distinguish up to 7 distinct rate constants  $R_{LLS}^{(\mu)}$  with  $\mu = AA',$   
190  $MM', XX', AA'MM', AA'XX', MM'XX'$  and  $AA'MM'XX'$ . Each term can be excited with a different amplitude and can contribute with a different weight to the observed signal.

In systems such as compounds III and IV with only two CH<sub>2</sub> groups, only one LLS can be excited:

$$\hat{\sigma}_{LLS} = (-\lambda_{AA'} \hat{\mathbf{I}}^A \cdot \hat{\mathbf{I}}^{A'} - \lambda_{XX'} \hat{\mathbf{I}}^X \cdot \hat{\mathbf{I}}^{X'}) - \lambda_{AA'XX'} (\hat{\mathbf{I}}^A \cdot \hat{\mathbf{I}}^{A'}) (\hat{\mathbf{I}}^X \cdot \hat{\mathbf{I}}^{X'}), \quad (4)$$

The coefficients of the first two bilinear terms are always equal, i.e.,  $\lambda_{AA'} = \lambda_{XX'}$  while the 4-spin term is always proportional to the leading bilinear terms, with a weight  $\lambda_{AA'XX'} = 8/3 \lambda_{AA'}$  (Sonnefeld et al., 2022a). This state corresponds to the  
195 imbalance between the singlet-singlet state and the triplet-triplet manifold and is therefore expected to decay monoexponentially. In two sets of complementary experiments performed for compound IV, the experimental relaxation rate constants were indeed found to be indistinguishable, as can be seen by comparing the red triangles and the green inverted triangles in Figure 4d.

In compounds I and II however, which contain three adjacent CH<sub>2</sub> groups, different SLIC excitation schemes lead to  
200 populate different LLS, with different coefficients  $\lambda_{LLS}^{(\mu)}$  in Eq. (3). There are 9 different ways of exciting miscellaneous LLS and 9 different ways of reconverting them, giving 81 possible experimental combinations. In order to investigate the relaxivities of these different LLS which may have different decay rate constants  $R_{LLS}^{(\mu)}$  and different relaxivities  $r_{LLS}^{(\mu)}$ , we performed 6 different poly-SLIC experiments with different SLIC pulses for excitation and reconversion, and indeed found different LLS lifetimes (Figure 5). Depending on the excitation and reconversion scheme used, there are pronounced differences between  
205 the relaxivities  $r_{LLS}$  within one and the same molecule.



210 **Figure 5. Decay rate constants  $R_{LLS}=1/T_{LLS}$  of long-lived states in  $\text{CH}_2$  groups in (a) DSS (I) and (b) homotaurine (II), each containing three  $\text{CH}_2$  groups, as a function of the TEMPOL concentration. Six different poly-SLIC experiments with distinct excitation and reconversion methods were performed for each molecule, as indicated by wavy arrows. The relaxivities  $r_{LLS}$  correspond to the slopes of the linear regressions.**

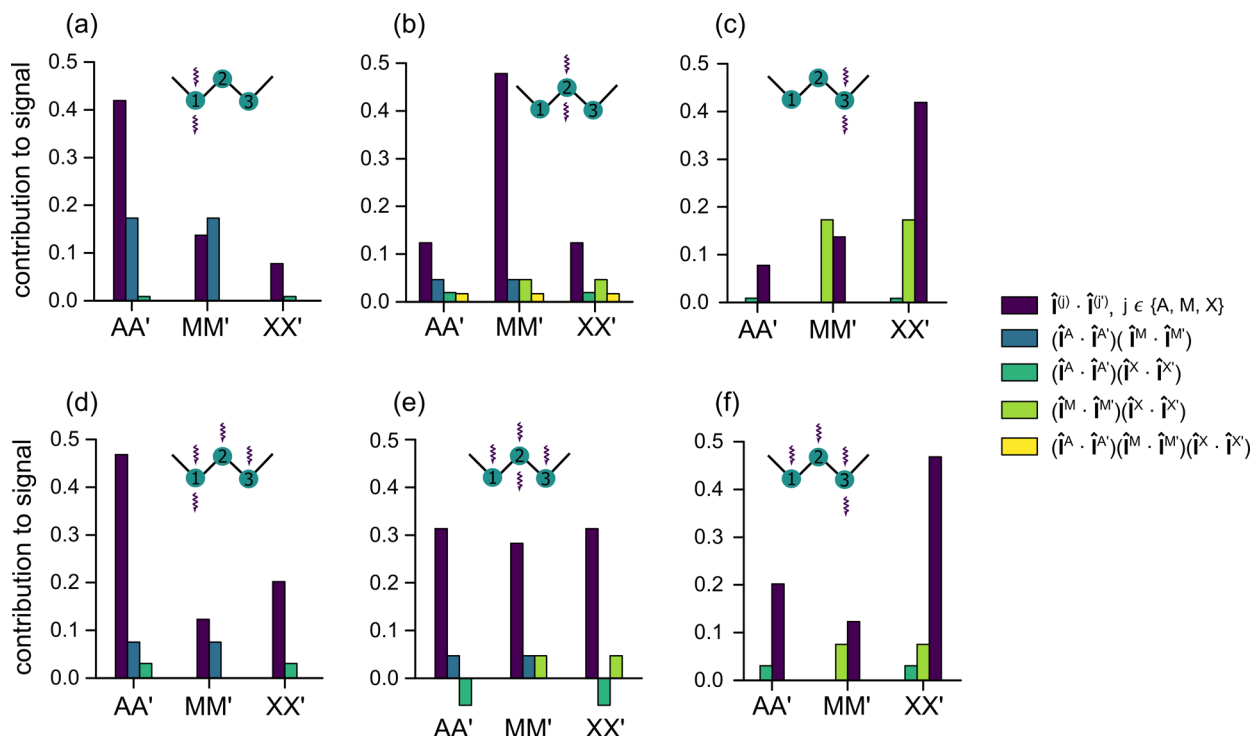
We calculated the contributions of each of the 7 terms to the observable LLS-derived signals, after two consecutive transformations  $\hat{I}_z^{in} \rightarrow \hat{\sigma}_{LLS} \rightarrow \hat{I}_x^{obs}$  (see Figure 6). For each excitation scheme used in this work, we considered all 7 coefficients  $\lambda_{\mu}^{M \rightarrow LLS}$  corresponding to the 7 terms in Eq. (3), as well as all 7 reconversion coefficients  $\tilde{\lambda}_{\mu}^{LLS \rightarrow M}$ . The coefficients are calculated according to:

$$\lambda_{\mu}^{M \rightarrow LLS}(\hat{I}_z^{in} \rightarrow \hat{\sigma}_{LLS}) = \frac{\text{Tr}\{\hat{P}_{\mu}^{\dagger} \cdot \hat{\sigma}_{LLS}\}}{\text{Tr}\{\hat{P}_{\mu}^{\dagger} \cdot \hat{P}_{\mu}\}},$$

$$\tilde{\lambda}_{\mu}^{LLS \rightarrow M}(\hat{P}_{\mu} \rightarrow \hat{I}_{x,\mu}^{obs}) = \frac{\text{Tr}\{\hat{I}_x^{\dagger} \cdot \hat{I}_{x,\mu}^{obs}\}}{\text{Tr}\{\hat{I}_x^{\dagger} \cdot \hat{I}_x\}},$$
(5)

215 where the index  $\mu$  corresponds to one of the 7 LLS terms in Eq. (3), the operator  $\hat{P}_{\mu}$  represents the  $\mu$ -th LLS term,  $\hat{I}_z^{in}$  is the initial magnetization of the excited spins,  $\hat{I}_x$  is the transverse magnetization of the observed spins after reconversion, and  $\hat{I}_{x,\mu}^{obs}$  is the transverse magnetization obtained after reconversion of only the  $\mu$ -th term  $\hat{P}_{\mu}$  instead of the full  $\hat{\sigma}_{LLS}$ . The observed signal  $S_{\mu}$  stemming from the  $\mu^{\text{th}}$  term is determined by the product of two coefficients  $\lambda_{\mu}^{M \rightarrow LLS}$  and  $\tilde{\lambda}_{\mu}^{LLS \rightarrow M}$  for a given combination of excitation and reconversion SLIC pulses. These contributions are shown in Figure 6. The sum of all 7 amplitudes for each

220 panel in Figure 6 was normalised to one. These graphs show how the LLS are delocalized across spin systems comprising  $n = 3$  neighboring  $\text{CH}_2$  groups. We only consider coherent spin dynamics during excitation and reconversion, neglecting possible redistributions of LLS due to Overhauser-type cross-relaxation effects, and neglecting zero-quantum coherences.



225 **Figure 6.** Calculated contributions of the 7 different LLS terms  $\hat{P}_\mu$  (the three two-spin terms are shown in the same colour) in the density operator of Eq. (3) to the observed signals for all 6 different single- and poly-SLIC experiments used in this work to determine the relaxivities  $r_{LLS}^{(a)}$  in the 6-spin systems of DSS (I) and homotaurine (II). The histograms show the products  $\lambda_\mu^{M \rightarrow LLS} \tilde{\lambda}_\mu^{LLS \rightarrow M}$  of the coefficients of LLS excitation and reconversion methods. The normalisation ensures that the sum of all products of coefficients is equal to 1. Experiments with triple SLIC excitation and single SLIC reconversion applied to the middle CH<sub>2</sub> group (e) provide LLS states that are almost evenly distributed among all three CH<sub>2</sub> groups, whereas the other experiments provide access to LLS states that are in part localised on the group where the reconversion SLIC pulse is applied. The excitation and reconversion of the (yellow) six-spin term is negligible except for case (b).  
230

Note that a *single* SLIC pulse applied at the chemical shift of *any* of the three CH<sub>2</sub> groups results in the excitation of a delocalized state, which is predominantly (but not exclusively) associated with the irradiated pair. By using triple SLIC excitation and single SLIC reconversion applied to the middle CH<sub>2</sub> group, one can excite a fairly even distribution of LLS  
235 involving all  $2n = 6$  coupled spins. For compound II, the most strongly delocalized state features the largest relaxivity  $r_{LLS}$ . For compound I, however, the largest relaxivities were obtained for experiments where the largest contribution to the observed signal came from the terminal group CH<sub>2</sub><sup>(3)</sup> that is closest to the trimethylsilane group. This group has also the largest longitudinal relaxivity  $r_1$ , as can be seen in Figure 4a. Detailed calculations of the relaxation superoperator might help to rationalize the experimental results obtained here.

## 240 **Conclusions**

The relaxation rate constants of various long-lived states and of the longitudinal magnetization of DSS, homotaurine, taurine and acetylcholine were measured as a function of the concentration of the radical TEMPOL. In all cases, the relaxivities  $r_{LLS}$  are lower by about a factor 3 compared to the relaxivities  $r_1$ . This implies that the effects of paramagnetic relaxation enhancement on LLS due to TEMPOL during sample transfer in dissolution DNP should not be too severe. Furthermore, the LLS relaxivity was studied for different SLIC excitation and reconversion schemes. The results support simulations that show that different LLS are excited depending on the SLIC sequence and the number of adjacent methylene units. SLIC methods have also been shown to be efficient for other achiral molecules containing neighboring CH<sub>2</sub> groups, such as dopamine,  $\gamma$ -aminobutyric acid (GABA), ethanolamine, and  $\beta$ -alanine (Sonnefeld, 2022a). All of these molecules contain aliphatic chains, so that the effects of paramagnetic polarizing agents like TEMPOL should be similar to what is reported in this work.

## 250 **Data availability**

All original NMR data obtained for this paper is available through the Zenodo repository under <https://doi.org/10.5281/zenodo.7432635>

## **Conflict of interest**

Geoffrey Bodenhausen is a member of the editorial board of the journal Magnetic Resonance of the Groupement Ampere. The peer-review process was guided by an independent editor. The authors do not have any other conflicting interests to declare.

## **Acknowledgements**

We are indebted to the CNRS and the ENS for support, and to the European Research Council (ERC) for the Synergy grant “Highly Informative Drug Screening by Overcoming NMR Restrictions” (HISCORE, grant agreement number 951459).

## **References**

- 260 Ardenkjær-Larsen, J. H., Fridlund, B., Gram, A., Hansson, G., Hansson, L., Lerche, M. H., Servin, R., Thaning, M., and Golman, K.: Increase in signal-to-noise ratio of  $> 10,000$  times in liquid-state NMR, PNAS, 100, 10158–10163, <https://doi.org/10.1073/pnas.1733835100>, 2003.
- Bengs, C. and Levitt, M. H.: SpinDynamica: Symbolic and numerical magnetic resonance in a Mathematica environment, Magn. Reson. Chem., 56, 374–414, <https://doi.org/10.1002/mrc.4642>, 2018.
- 265 Borah, B. and Bryant, R. G.: NMR relaxation dispersion in an aqueous nitroxide system, J. Chem. Phys., 75, 3297–3300, <https://doi.org/10.1063/1.442480>, 1981.

- Bornet, A., Ji, X., Mammoli, D., Vuichoud, B., Milani, J., Bodenhausen, G., and Jannin, S.: Long-Lived States of Magnetically Equivalent Spins Populated by Dissolution-DNP and Revealed by Enzymatic Reactions, *Eur. J. Chem.*, 20, 17113–17118, <https://doi.org/10.1002/chem.201404967>, 2014.
- 270 Buratto, R., Bornet, A., Milani, J., Mammoli, D., Vuichoud, B., Salvi, N., Singh, M., Laguerre, A., Passemard, S., Gerber-Lemaire, S., Jannin, S., and Bodenhausen, G.: Drug Screening Boosted by Hyperpolarized Long-Lived States in NMR, *ChemMedChem*, 9, 2509–2515, <https://doi.org/10.1002/cmdc.201402214>, 2014a.
- Buratto, R., Mammoli, D., Chiarparin, E., Williams, G., and Bodenhausen, G.: Exploring Weak Ligand–Protein Interactions by Long-Lived NMR States: Improved Contrast in Fragment-Based Drug Screening, *Angew. Chem. Int. Ed.*, 53, 11376–  
275 11380, <https://doi.org/10.1002/anie.201404921>, 2014b.
- Buratto, R., Mammoli, D., Canet, E., and Bodenhausen, G.: Ligand–Protein Affinity Studies Using Long-Lived States of Fluorine-19 Nuclei, *J. Med. Chem.*, 59, 1960–1966, <https://doi.org/10.1021/acs.jmedchem.5b01583>, 2016.
- Carravetta, M. and Levitt, M. H.: Long-Lived Nuclear Spin States in High-Field Solution NMR, *J. Am. Chem. Soc.*, 126, 6228–6229, <https://doi.org/10.1021/ja0490931>, 2004.
- 280 Carravetta, M., Johannessen, O. G., and Levitt, M. H.: Beyond the T1 Limit: Singlet Nuclear Spin States in Low Magnetic Fields, *Phys. Rev. Lett.*, 92, 153003, <https://doi.org/10.1103/PhysRevLett.92.153003>, 2004.
- DeVience, S. J., Walsworth, R. L., and Rosen, M. S.: Preparation of Nuclear Spin Singlet States Using Spin-Lock Induced Crossing, *Phys. Rev. Lett.*, 111, 173002, <https://doi.org/10.1103/PhysRevLett.111.173002>, 2013.
- Eichhorn, T. R., Takado, Y., Salameh, N., Capozzi, A., Cheng, T., Hyacinthe, J.-N., Mishkovsky, M., Roussel, C., and  
285 Comment, A.: Hyperpolarization without persistent radicals for in vivo real-time metabolic imaging, *PNAS*, 110, 18064–18069, <https://doi.org/10.1073/pnas.1314928110>, 2013.
- El Daraï, T., Cousin, S. F., Stern, Q., Ceillier, M., Kempf, J., Eshchenko, D., Melzi, R., Schnell, M., Gremillard, L., Bornet, A., Milani, J., Vuichoud, B., Cala, O., Montarnal, D., and Jannin, S.: Porous functionalized polymers enable generating and transporting hyperpolarized mixtures of metabolites, *Nat. Commun.*, 12, 4695, <https://doi.org/10.1038/s41467-021-24279-2>,  
290 2021.
- Elliott, S. J., Kadeřávek, P., Brown, L. J., Sabba, M., Glöggler, S., O’Leary, D. J., Brown, R. C. D., Ferrage, F., and Levitt, M. H.: Field-cycling long-lived-state NMR of  $^{15}\text{N}_2$  spin pairs, *Mol. Phys.*, 117, 861–867, <https://doi.org/10.1080/00268976.2018.1543906>, 2019.
- Erriah, B. and Elliott, S. J.: Experimental evidence for the role of paramagnetic oxygen concentration on the decay of long-  
295 lived nuclear spin order, *RSC Adv.*, 9, 23418–23424, <https://doi.org/10.1039/C9RA03748A>, 2019.
- Feng, Y., Theis, T., Liang, X., Wang, Q., Zhou, P., and Warren, W. S.: Storage of Hydrogen Spin Polarization in Long-Lived  $^{13}\text{C}_2$  Singlet Order and Implications for Hyperpolarized Magnetic Resonance Imaging, *J. Am. Chem. Soc.*, 135, 9632–9635, <https://doi.org/10.1021/ja404936p>, 2013.
- Franzoni, M. B., Buljubasich, L., Spiess, H. W., and Münnemann, K.: Long-Lived  $^1\text{H}$  Singlet Spin States Originating from Para-Hydrogen in Cs-Symmetric Molecules Stored for Minutes in High Magnetic Fields, *J. Am. Chem. Soc.*, 134, 10393–  
300 10396, <https://doi.org/10.1021/ja304285s>, 2012.
- Gajan, D., Bornet, A., Vuichoud, B., Milani, J., Melzi, R., van Kalkeren, H. A., Veyre, L., Thieuleux, C., Conley, M. P., Grüning, W. R., Schwarzwälder, M., Lesage, A., Copéret, C., Bodenhausen, G., Emsley, L., and Jannin, S.: Hybrid polarizing

- solids for pure hyperpolarized liquids through dissolution dynamic nuclear polarization, *PNAS*, 111, 14693–14697, 305 <https://doi.org/10.1073/pnas.1407730111>, 2014.
- Hogben, H. J., Hore, P. J., and Kuprov, I.: Multiple decoherence-free states in multi-spin systems, *J. Magn. Reson.*, 211, 217–220, <https://doi.org/10.1016/j.jmr.2011.06.001>, 2011.
- Ji, X., Bornet, A., Vuichoud, B., Milani, J., Gajan, D., Rossini, A. J., Emsley, L., Bodenhausen, G., and Jannin, S.: Transportable hyperpolarized metabolites, *Nat. Commun.*, 8, 13975, <https://doi.org/10.1038/ncomms13975>, 2017.
- 310 Kharkov, B., Duan, X., Rantaharju, J., Sabba, M., Levitt, M. H., Canary, J. W., and Jerschow, A.: Weak nuclear spin singlet relaxation mechanisms revealed by experiment and computation, *Phys. Chem. Chem. Phys.*, 24, 7531–7538, <https://doi.org/10.1039/D1CP05537B>, 2022.
- Kim, Y., Liu, M., and Hilty, C.: Parallelized Ligand Screening Using Dissolution Dynamic Nuclear Polarization, *Anal. Chem.*, 88, 11178–11183, <https://doi.org/10.1021/acs.analchem.6b03382>, 2016.
- 315 Kiryutin, A. S., Rodin, B. A., Yurkovskaya, A. V., Ivanov, K. L., Kurzbach, D., Jannin, S., Guarin, D., Abergel, D., and Bodenhausen, G.: Transport of hyperpolarized samples in dissolution-DNP experiments, *Phys. Chem. Chem. Phys.*, 21, 13696–13705, <https://doi.org/10.1039/C9CP02600B>, 2019.
- Kouřil, K., Kouřilová, H., Bartram, S., Levitt, M. H., and Meier, B.: Scalable dissolution-dynamic nuclear polarization with rapid transfer of a polarized solid, *Nat. Commun.*, 10, 1733, <https://doi.org/10.1038/s41467-019-09726-5>, 2019.
- 320 Kress, T., Walrant, A., Bodenhausen, G., and Kurzbach, D.: Long-Lived States in Hyperpolarized Deuterated Methyl Groups Reveal Weak Binding of Small Molecules to Proteins, *J. Phys. Chem. Lett.*, 10, 1523–1529, <https://doi.org/10.1021/acs.jpcclett.9b00149>, 2019.
- Lee, Y., Zeng, H., Ruedisser, S., Gossert, A. D., and Hilty, C.: Nuclear Magnetic Resonance of Hyperpolarized Fluorine for Characterization of Protein–Ligand Interactions, *J. Am. Chem. Soc.*, 134, 17448–17451, <https://doi.org/10.1021/ja308437h>, 325 2012.
- Miéville, P., Ahuja, P., Sarkar, R., Jannin, S., Vasos, P. R., Gerber-Lemaire, S., Mishkovsky, M., Comment, A., Gruetter, R., Ouari, O., Tordo, P., and Bodenhausen, G.: Scavenging Free Radicals To Preserve Enhancement and Extend Relaxation Times in NMR using Dynamic Nuclear Polarization, *Angew. Chem. Int. Ed.*, 49, 6182–6185, <https://doi.org/10.1002/anie.201000934>, 2010.
- 330 Miéville, P., Jannin, S., and Bodenhausen, G.: Relaxometry of insensitive nuclei: Optimizing dissolution dynamic nuclear polarization, *J. Magn. Reson.*, 210, 137–140, <https://doi.org/10.1016/j.jmr.2011.02.006>, 2011.
- Negrone, M., Turhan, E., Kress, T., Ceillier, M., Jannin, S., and Kurzbach, D.: Frémy’s Salt as a Low-Persistence Hyperpolarization Agent: Efficient Dynamic Nuclear Polarization Plus Rapid Radical Scavenging, *J. Am. Chem. Soc.*, 144, 20680–20686, <https://doi.org/10.1021/jacs.2c07960>, 2022.
- 335 Nelson, S. J., Kurhanewicz, J., Vigneron, D. B., Larson, P. E. Z., Harzstark, A. L., Ferrone, M., van Criekinge, M., Chang, J. W., Bok, R., Park, I., Reed, G., Carvajal, L., Small, E. J., Munster, P., Weinberg, V. K., Ardenkjaer-Larsen, J. H., Chen, A. P., Hurd, R. E., Odegardstuen, L.-I., Robb, F. J., Tropp, J., and Murray, J. A.: Metabolic Imaging of Patients with Prostate Cancer Using Hyperpolarized [1-<sup>13</sup>C]Pyruvate, *Sci. Transl. Med.*, 5, 198ra108, <https://doi.org/10.1126/scitranslmed.3006070>, 2013.

- 340 Pileio, G., Hill-Cousins, J. T., Mitchell, S., Kuprov, I., Brown, L. J., Brown, R. C. D., and Levitt, M. H.: Long-Lived Nuclear Singlet Order in Near-Equivalent  $^{13}\text{C}$  Spin Pairs, *J. Am. Chem. Soc.*, 134, 17494–17497, <https://doi.org/10.1021/ja3089873>, 2012.
- Salvi, N., Buratto, R., Bornet, A., Ulzega, S., Rentero Rebollo, I., Angelini, A., Heinis, C., and Bodenhausen, G.: Boosting the Sensitivity of Ligand–Protein Screening by NMR of Long-Lived States, *J. Am. Chem. Soc.*, 134, 11076–11079, <https://doi.org/10.1021/ja303301w>, 2012.
- 345 Sarkar, R., Vasos, P. R., and Bodenhausen, G.: Singlet-State Exchange NMR Spectroscopy for the Study of Very Slow Dynamic Processes, *J. Am. Chem. Soc.*, 129, 328–334, <https://doi.org/10.1021/ja0647396>, 2007.
- Sheberstov, K. F., Vieth, H.-M., Zimmermann, H., Rodin, B. A., Ivanov, K. L., Kiryutin, A. S., and Yurkovskaya, A. V.: Generating and sustaining long-lived spin states in  $^{15}\text{N}$ ,  $^{15}\text{N}'$ -azobenzene, *Sci. Rep.*, 9, 20161, <https://doi.org/10.1038/s41598-019-56734-y>, 2019.
- 350 Sonnefeld, A., Razanahoera, A., Pelupessy, P., Bodenhausen, G., and Sheberstov, K.: Long-lived states of methylene protons in achiral molecules, *Sci. Adv.*, 8, eade2113, <https://doi.org/10.1126/sciadv.ade2113>, 2022a.
- Sonnefeld, A., Bodenhausen, G., and Sheberstov, K.: Polychromatic Excitation of Delocalized Long-Lived Proton Spin States in Aliphatic Chains, *Phys. Rev. Lett.*, 129, 183203, <https://doi.org/10.1103/PhysRevLett.129.183203>, 2022b.
- 355 Stevanato, G., Hill-Cousins, J. T., Håkansson, P., Roy, S. S., Brown, L. J., Brown, R. C. D., Pileio, G., and Levitt, M. H.: A Nuclear Singlet Lifetime of More than One Hour in Room-Temperature Solution, *Angew. Chem. Int. Ed.*, 54, 3740–3743, <https://doi.org/10.1002/anie.201411978>, 2015.
- Tayler, M. C. D.: Chapter 10: Filters for Long-lived Spin Order, in: *Long-lived Nuclear Spin Order*, The Royal Society of Chemistry, 188–208, <https://doi.org/10.1039/9781788019972-00188>, 2020.
- 360 Tayler, M. C. D. and Levitt, M. H.: Paramagnetic relaxation of nuclear singlet states, *Phys. Chem. Chem. Phys.*, 13, 9128–9130, <https://doi.org/10.1039/C1CP20471H>, 2011.
- Tayler, M. C. D. and Levitt, M. H.: Accessing Long-Lived Nuclear Spin Order by Isotope-Induced Symmetry Breaking, *J. Am. Chem. Soc.*, 135, 2120–2123, <https://doi.org/10.1021/ja312227h>, 2013.
- 365 Tayler, M. C. D., Marco-Rius, I., Kettunen, M. I., Brindle, K. M., Levitt, M. H., and Pileio, G.: Direct Enhancement of Nuclear Singlet Order by Dynamic Nuclear Polarization, *J. Am. Chem. Soc.*, 134, 7668–7671, <https://doi.org/10.1021/ja302814e>, 2012.
- Wokaun, A. and Ernst, R. R.: The use of multiple quantum transitions for relaxation studies in coupled spin systems, *Mol. Phys.*, 36, 317–341, <https://doi.org/10.1080/00268977800101601>, 1978.